Characterisation of intermediates involved in the *mer*-W(CO)$_3$(η^1-dpm)(η^2-dpm) to *mer*-[W(CO)$_2$(η^2-dpm)$_2$]$^{2+}$ (dpm = Ph$_2$PCH$_2$PPh$_2$) oxidation process in acetone by steady-state and fast scan voltammetry at platinum and mercury microelectrodes

Alan M. Bond*, Ray Colton
Department of Chemistry, La Trobe University, Bundoora 3083 (Australia)

and Roger S. Hutton**
Inorganic Chemistry Section, School of Chemistry, University of Melbourne, Parkville 3052 (Australia)

Abstract

The oxidation of *mer*-W(CO)$_3$(η^1-dpm)(η^2-dpm) (dpm = Ph$_2$PCH$_2$PPh$_2$) under conventional voltammetric conditions is known to involve an overall two-electron oxidation process to give [W(CO)$_3$(η^2-dpm)$_2$]$^{2+}$ with no experimental evidence for postulated intermediates. Under steady-state or near steady-state conditions at platinum microelectrodes with radii greater than 25 μm the oxidation of *mer*-W(CO)$_3$(η^1-dpm)(η^2-dpm) is observed to still proceed via a single two-electron process whereas at a 3 μm radius microelectrode two one-electron processes are observed. This dependence upon electrode size is consistent with a mechanism involving single electron transfer steps and internal chelating reactions. The first electron transfer step is *mer*-W(CO)$_3$(η^1-dpm)(η^2-dpm) $\rightleftharpoons$ *mer*-[W(CO)$_3$(η^1-dpm)(η^2-dpm)]$^+$ + e^- (reaction a). Following this initial oxidation there are two competing pathways to further oxidation: *mer*-[W(CO)$_3$(η^1-dpm)(η^2-dpm)]$^+$ $\rightarrow$ *mer*-[W(CO)$_3$(η^2-dpm)$_2$]$^+$ (b) followed by *mer*-[W(CO)$_3$(η^2-dpm)$_2$]$^+$ $\rightarrow$ [W(CO)$_3$(η^2-dpm)$_2$]$^{2+}$ + e^- (c) or *mer*-[W(CO)$_3$(η^1-dpm)(η^2-dpm)]$^+$ $\rightleftharpoons$ *mer*-[W(CO)$_3$(η^1-dpm)(η^2-dpm)]$^{2+}$ + e^- (d) followed by *mer*-[W(CO)$_3$(η^1-dpm)(η^2-dpm)]$^{2+}$ $\rightarrow$ [W(CO)$_3$(η^2-dpm)$_2$]$^{2+}$ (e). Under conventional voltammetric conditions reaction sequence (a), (b), (c) gives rise to a single apparent two-electron process. Two one-electron processes are observed when the internal chelation step is outrun by the short time scale achieved under steady-state conditions or by very fast transient voltammetry at platinum microelectrodes. The fast scan rate technique provides direct evidence for the fleeting existence of the seventeen-electron *mer*-[W(CO)$_3$(η^1-dpm)(η^2-dpm)]$^+$ and the nineteen-electron [W(CO)$_3$(η^2-dpm)$_2$]$^+$ species. The complementary nature of the steady-state and transient regimes of voltammetry at microelectrodes is therefore demonstrated by the present study. The mechanism of the electrochemical oxidation of *mer*-W(CO)$_3$(η^1-dpm)(η^2-dpm) at gold and carbon electrodes appears to be the same as at platinum. In contrast, at both conventional and microsized mercury electrodes weak interaction of the pendent phosphorus atom of *mer*-W(CO)$_3$(η^1-dpm)(η^2-dpm) with mercury effectively slows down the rate of chelation following oxidation. Thus voltammetry at a mercury electrode allows the two one-electron oxidation steps for *mer*-W(CO)$_3$(η^1-dpm)(η^2-dpm) to be observed under conventional voltammetric conditions. It is concluded therefore, that in the presence of a pendent phosphorus group, mercury electrode interaction provides another convenient method of studying unstable intermediates via what may be referred to as a surface trapping technique.

Introduction

The electrochemical oxidations of six-coordinate eighteen-electron carbonyl compounds of the Group 6 metals (Cr, Mo, W) containing monodentate and bidentate phosphine ligands have been thoroughly investigated. The sixteen- or seventeen-electron species
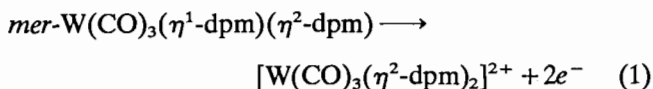
generated by oxidation are usually labile and isomerisation, disproportionation, dissociation, cross redox and self-exchange reactions accompanying electron transfer have been identified [1–11]. Recent work in our laboratories [7] has shown that when a pendent ligand is present, such as in the case of *mer*-W(CO)$_3$(η^1-dpm)(η^2-dpm) (dpm = Ph$_2$PCH$_2$PPh$_2$), the reaction pathways of the oxidised product may be even more varied than for complexes containing only monodentate or chelated ligands, since the η^1-dpm ligand may become chelated after oxidation. However, the identification of inter-

---

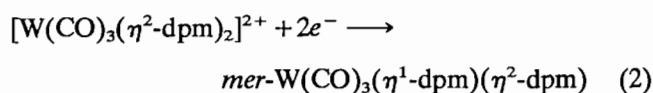*Author to whom correspondence should be addressed.
**Present address: Department of Chemistry, The University, Southampton S02 5NH, UK.

mediates in the oxidation reaction is difficult when the rates of the homogeneous reactions accompanying the electron transfer are fast.

In the particular case of mer-$W(CO)_3(\eta^1$-dpm$)(\eta^2$-dpm$)$ the electrochemistry has been investigated in acetone and dichloromethane solution at conventionally sized electrodes [7]. This compound was found to undergo a two-electron oxidation at a platinum electrode to give $[W(CO)_3(\eta^2$-dpm$)_2]^{2+}$ (eqn. (1))

$$mer\text{-}W(CO)_3(\eta^1\text{-dpm})(\eta^2\text{-dpm}) \longrightarrow$$
$$[W(CO)_3(\eta^2\text{-dpm})_2]^{2+} + 2e^- \quad (1)$$

which could be reduced by a two-electron step back to mer-$W(CO)_3(\eta^1$-dpm$)(\eta^2$-dpm$)$ (eqn. (2))

$$[W(CO)_3(\eta^2\text{-dpm})_2]^{2+} + 2e^- \longrightarrow$$
$$mer\text{-}W(CO)_3(\eta^1\text{-dpm})(\eta^2\text{-dpm}) \quad (2)$$

where the potentials of the oxidation and reduction are separated by 0.70 V indicating the processes are electrochemically irreversible in the Nernstian sense, even though the overall reaction is chemically reversible. Although intermediates such as mer-$[W(CO)_3(\eta^1$-dpm$)(\eta^2$-dpm$)]^+$ and mer-$[W(CO)_3(\eta^1$-dpm$)(\eta^2$-dpm$)]^{2+}$ were postulated [7] no proof for their existence was obtained.

In this work, both steady-state and fast scan rate voltammetry at platinum and mercury microelectrodes is employed to illustrate how reaction intermediates associated with the redox processes in eqns. (1) and (2) may be identified.

Experimental

Materials
The complex mer-$W(CO)_3(\eta^1$-dpm$)(\eta^2$-dpm$)$ was prepared according to literature methods [7, 12].

Electrochemistry
Cyclic voltammetry at a conventional macrosized platinum electrode of radius 0.31 cm was performed in a standard three-electrode cell by using a model 174 E.G. and G. PAR electrochemical system. Potentials were measured relative to a Ag/AgCl (CH_2Cl_2; saturated LiCl) reference electrode which was separated from the test solution by a salt bridge containing 0.1 M Et_4NClO_4 in acetone.

Microelectrode studies were conducted with a two-electrode cell geometry by using a Cypress Systems CYSY-1 electrochemistry system at scan rates up to 200 V s^{-1}. Platinum and gold microelectrodes were fabricated according to literature methods [13] whilst the glassy carbon electrode (radius 5 μm) was purchased from E.G. and G. PAR. Mercury microelectrodes were

prepared using the following procedure. A platinum microdisc electrode was soaked in concentrated nitric acid and then washed with distilled water. Mercury was nucleated onto the platinum surface from an aqueous solution of $Hg_2(NO_3)_2$ (acidified to pH 3.0 with HNO_3) by controlled potential electrolysis at -300 mV versus a mercury pool reference electrode. The resulting mercury microelectrode was then allowed to stand in acetone for at least ten minutes before use. The size of each mercury microelectrode was calculated by three independent methods: (i) from the charge transferred during nucleation; (ii) by measuring the diffusion controlled limiting current in a standard solution of ferrocene in acetone; (iii) by oxidative stripping analysis. The sizes of the microelectrodes determined by all three methods were in close agreement. In all cases it was assumed that a hemispherical geometry is appropriate for a mercury microelectrode attached to a platinum disc and that the mercury electrode was much larger than the platinum disc [14]. A platinum wire pseudoreference electrode was used in the microelectrode experiments.

All reference electrodes were frequently calibrated against a standard ferrocene (Fc) solution and all potentials are quoted relative to the Fc$^+$/Fc redox couple. All measurements unless otherwise stated were performed in acetone (0.1 M Et_4NClO_4) at 20 ± 2 °C with 0.5 mM mer-$W(CO)_3(\eta^1$-dpm$)(\eta^2$-dpm$)$. Platinum, gold and carbon electrodes were polished with 0.05 μm alumina/water slurries on a micropolishing cloth prior to each experiment and then rinsed with acetone. Oxygen was removed from all solutions by nitrogen bubbling prior to voltammetric measurements, and all experiments were performed under a nitrogen atmosphere.

Results and discussion

Steady-state voltammetry at platinum microelectrodes
Figure 1(a) shows a cyclic voltammogram for mer-$W(CO)_3(\eta^1$-dpm$)(\eta^2$-dpm$)$ at a conventionally sized platinum disc electrode (radius 0.31 cm) at a scan rate of 0.1 V s^{-1}. Under these transient voltammetric conditions where mass transport is controlled by linear diffusion, the two processes correspond to eqns. (1) and (2) [7]. At this size electrode currents are in the microampere range and the ohmic IR drop is substantial. Figure 1(b) shows the near steady-state response which is obtained at slow scan rates at a platinum disc microelectrode with a radius of 25 μm. Currents are now in the nanoampere region and neither the IR drop nor the charging current present any problems under these steady-state conditions. However, since radial, rather than linear, diffusion is now the dominant mode of mass transport, a predominantly sigmoidal shaped oxidation curve is observed (process 1, $E_{1/2} = -0.14$ V
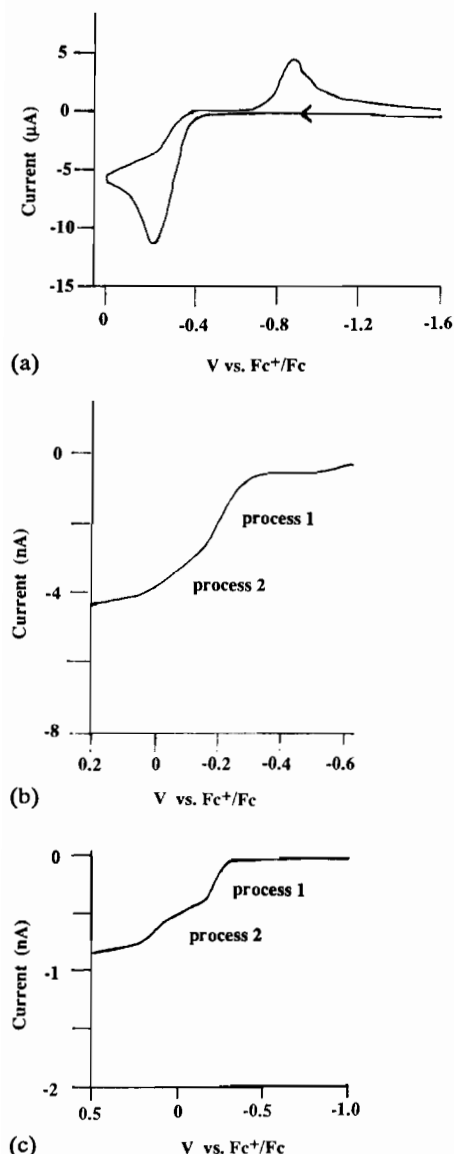
Fig. 1. Oxidative cyclic voltammograms (scan rate = 0.1 V s^{-1}) for a 0.5 mM solution of *mer*-W(CO)$_3$(η^1-dpm)(η^2-dpm) in acetone (0.1 M Et$_4$NClO$_4$) at various sized platinum disc electrodes: (a) 0.31 cm, (b) 25 μm, (c) 3 μm.

where n is the number of electrons transferred in the redox process, F is the Faraday constant, C the concentration of electroactive species in the bulk solution, D the diffusion coefficient and r the radius of the microdisc. The radius of each microelectrode was determined from the diffusion controlled limiting currents obtained with a standard solution of ferrocene in acetonitrile using eqn. (3) [16]. In order to determine the number of electrons involved in processes 1 and 2 preliminary measurements were made with the compounds *fac*- and *mer*-Cr(CO)$_3$(η^1-dpe)(η^2-dpe) (dpe = Ph$_2$PCH$_2$CH$_2$PPh$_2$) which are each known to undergo a one-electron reversible oxidation. Using eqn. (3) and the calibrated microelectrodes, absolute values of $(4.2 \pm 0.7) \times 10^{-6}$ and $(4.2 \pm 0.6) \times 10^{-6}$ cm^2 s^{-1} were determined for the diffusion coefficients of the *fac* and *mer* isomers, respectively. Then, assuming that a similar diffusion coefficient is applicable to *mer*-W(CO)$_3$(η^1-dpm)(η^2-dpm), the number of electrons in processes 1 and 2 may be calculated from the measured diffusion current for this compound. Analysis of the data in this manner reveals that at the 25 μm radius microelectrode (Fig. 1(b)) process 1 corresponds almost to a two-electron response. In contrast, at the 3 μm radius microelectrode (Fig. 1(c)) the response consists approximately of two one-electron processes. At intermediate electrode radii, the apparent number of electrons for process 1 is greater than one and that for process 2 is less than one, with their sum always being two. A value of $(4.0 \pm 0.6) \times 10^{-6}$ cm^2 s^{-1} was obtained for the diffusion coefficient of *mer*-W(CO)$_3$(η^1-dpm)(η^2-dpm) in acetone assuming that the total diffusion controlled limiting current corresponds to an exact two-electron process.

The above results show that steady-state voltammetry at microelectrodes provides evidence for the existence of intermediates which cannot be detected by conventional voltammetry. The oxidation of *mer*-W(CO)$_3$(η^1-dpm)(η^2-dpm) to the characterised [17] eighteen-electron species [W(CO)$_3$(η^2-dpm)$_2$]$^{2+}$ may in principle be rationalised by several pathways according to the data obtained under steady-state or near steady-state conditions at platinum electrodes. The rate of chelation of the initially mondentate dpm ligand and the time scale of the electrochemical experiment determine whether one two-electron or two one-electron steps are observed. The pathways termed ECE and EE'C reactions, using the notation of Feldberg and Jeftic [18], may also be combined with a disproportionation reaction.

(a) ECE mechanism (process 1)

mer-W(CO)$_3$(η^1-dpm)(η^2-dpm) $\rightleftharpoons$

$$\textit{mer}\text{-}[\text{W(CO)}_3(\eta^1\text{-dpm})(\eta^2\text{-dpm})]^+ + e^- \quad (4a)$$

versus Fc$^+$/Fc). A second small oxidation process at approximately 0.08 V versus Fc$^+$/Fc (process 2) is barely distinguishable from the background. At a smaller 12.6 μm radius platinum disc microelectrode the response approximates more closely to steady-state conditions and process 2 is more clearly seen. At a 3 μm radius microelectrode two separate oxidation processes with approximately equal limiting currents are observed (Fig. 1(c)).

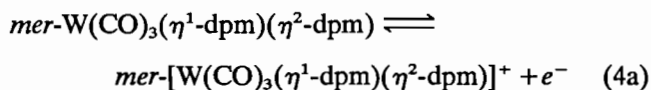The radial diffusion controlled limiting current i_d at an inlaid disc microelectrode [15] is given by eqn. (3)
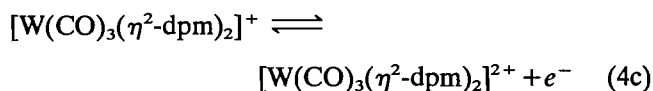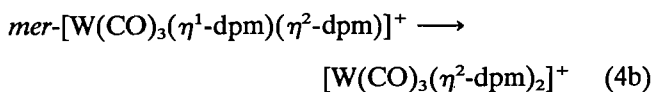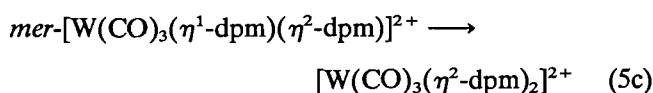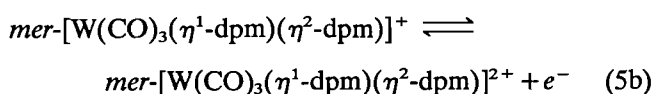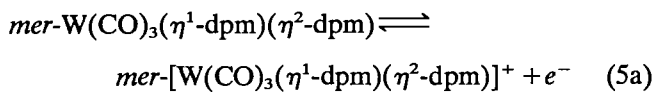
$$i_d = 4nFCDr \quad (3)$$

mer-[W(CO)$_3$(η^1-dpm)(η^2-dpm)]$^+$ $\longrightarrow$

$$[W(CO)_3(\eta^2\text{-dpm})_2]^+ \quad (4b)$$

[W(CO)$_3$(η^2-dpm)$_2$]$^+$ $\rightleftharpoons$

$$[W(CO)_3(\eta^2\text{-dpm})_2]^{2+} + e^- \quad (4c)$$

(b) EE'C mechanism (when process 2 is observed)

mer-W(CO)$_3$(η^1-dpm)(η^2-dpm) $\rightleftharpoons$

$$mer\text{-}[W(CO)_3(\eta^1\text{-dpm})(\eta^2\text{-dpm})]^+ + e^- \quad (5a)$$

mer-[W(CO)$_3$(η^1-dpm)(η^2-dpm)]$^+$ $\rightleftharpoons$

$$mer\text{-}[W(CO)_3(\eta^1\text{-dpm})(\eta^2\text{-dpm})]^{2+} + e^- \quad (5b)$$

mer-[W(CO)$_3$(η^1-dpm)(η^2-dpm)]$^{2+}$ $\longrightarrow$

$$[W(CO)_3(\eta^2\text{-dpm})_2]^{2+} \quad (5c)$$

(c) EC (disproportionation)

mer-W(CO)$_3$(η^1-dpm)(η^2-dpm) $\rightleftharpoons$

$$mer\text{-}[W(CO)_3(\eta^1\text{-dpm})(\eta^2\text{-dpm})]^+ + e^- \quad (6a)$$

2*mer*-[W(CO)$_3$(η^1-dpm)(η^2-dpm)]$^+$ $\longrightarrow$

mer-W(CO)$_3$(η^1-dpm)(η^2-dpm) + [W(CO)$_3$(η^2-dpm)$_2$]$^{2+}$

$$(6b)$$
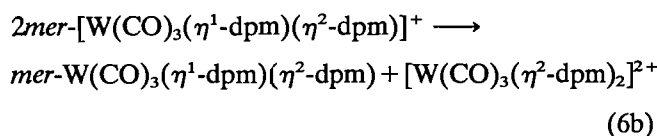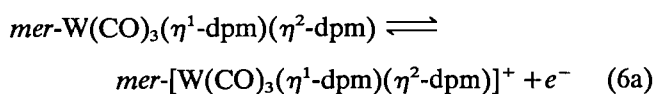
In principle, the steady-state responses observed as a function of electrode size may be explained by both the ECE (eqn. (4)) and EE'C (eqn. (5)) mechanisms with disproportionation (eqn. (6b)) possibly also being involved. Assuming the disproportionation reaction is operative and is described by second or higher order kinetics, then the steady-state behaviour at microelectrodes in the intermediate radius regime (25 μm > r > 3 μm) should be dependent upon the concentration of *mer*-W(CO)$_3$(η^1-dpm)(η^2-dpm). Thus, in this case it would be predicted that the relative heights of processes 1 and 2 would be concentration dependent. Data obtained over the concentration range 0.5–10 mM at a 5 μm radius microelectrode show that the ratio of heights of processes 1 and 2 is, within experimental error, independent of concentration. It is therefore concluded that the disproportionation reaction (eqn. (6b)) is unimportant, at least on the time scale of these experiments.

The behaviour observed as a function of electrode size may now be explained as follows via the ECE and EE'C mechanisms. At the 0.3 μm radius microelectrode, the chelation step following the first one-electron transfer is too slow to influence the response on the time scale associated with this size electrode. Under these conditions, process 1 is a simple reversible one-electron process (eqn. (4a)) and process 2 corresponds to an EE'C reaction with chelation occurring after the second electron transfer process (eqn. (5b, c)). At larger electrodes, only a single two-electron process is observed because only the ECE process 1 is operative, which requires that the potential of step (4c) is less positive than (4a). This assumption will be justified later.

The theory for the ECE process has been derived [19, 20] and it allows the rate of the first order chelation step (eqn. (4b)) to be calculated as 2×10^3 s^{-1} assuming that the diffusion to a microdisc electrode approximates that at a hemisphere. At gold and carbon microelectrodes steady-state behaviour was found to be identical to that at platinum.

Transient voltammetry at platinum microelectrodes

For conventionally sized electrodes using organic solvents such as acetone and with concentrations of electroactive species of 0.5 mM the upper scan rate available with cyclic voltammetry is about 5 V s^{-1}. At higher scan rates problems with IR drop and charging current lead to significant distortions. Microelectrodes provide a lower experimental time constant which allows a wider voltammetric time domain to be investigated and the use of microelectrodes reduces, but does not eliminate, IR drop effects. However, under transient conditions the effects of the charging current are not reduced at microelectrodes because the ratio of the charging current to the Faradaic current remains constant. The use of fast scan rates permits the direct study of electroactive compounds resulting from chemical reactions following electron transfer. Thus the transient data should be complementary to steady-state results, where products are swept away from the electrode surface and cannot be monitored directly. Linear diffusion becomes important at fast scan rates even with microelectrodes, so the chemistry of the products of electron transfer may be studied on the reverse scan of a cyclic voltammogram.

Figure 2 shows the voltammetric response for the oxidation of a 0.5 mM solution of *mer*-W(CO)$_3$(η^1-dpm)(η^2-dpm) in acetone (0.2 M Et$_4$NClO$_4$) as a function of scan rate at a 12.5 μm radius platinum microelectrode. At scan rates of 1 and 10 V s^{-1} (Fig. 2(a, b)) the voltammetric response changes from near steady-state to a mixture of steady-state and linear diffusion. At a scan rate of 100 V s^{-1} (Fig. 2(c)) linear diffusion is dominant and well defined peaks are observed on both the forward and reverse scans although unfortunately the charging current becomes large and masks some details of the Faradaic processes. At a 3 μm radius microelectrode, the radial diffusion terms are still important at 100 V s^{-1}, although the two one-electron oxidations do exhibit a partial peak shaped behaviour.
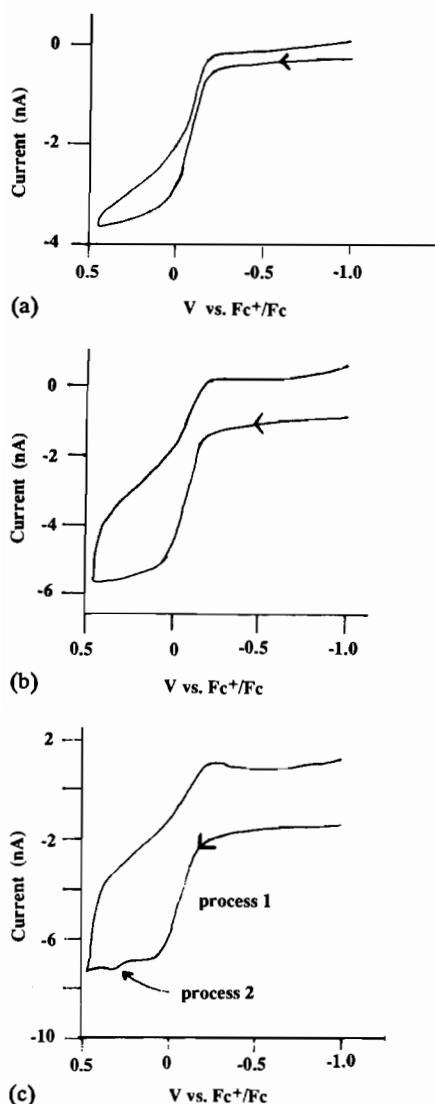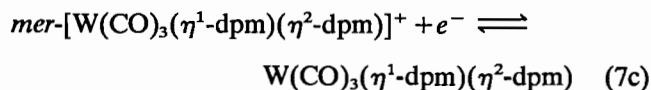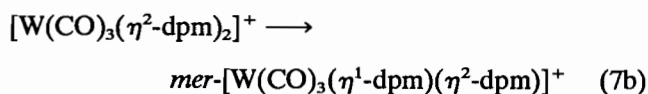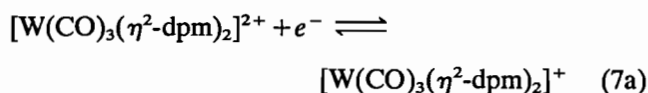
Fig. 2. Oxidative cyclic voltammograms for a 0.5 mM solution of *mer*-W(CO)$_3$(η^1-dpm)(η^2-dpm) in acetone (0.1 M Et$_4$NClO$_4$) at a 12.5 μm radius platinum disc microelectrode at different scan rates: (a) 1, (b) 10, (c) 100 V s^{-1}.

Despite the presence of considerable charging current, at scan rates of 100 V s^{-1} direct evidence for the chemically reversible reaction *mer*-W(CO)$_3$(η^1-dpm)(η^2-dpm) $\rightleftharpoons$ *mer*-[W(CO)$_3$(η^1-dpm)(η^2-dpm)]$^+$ + e^- is obtained since process 1 now has both oxidation and reduction peaks (Fig. 2(c)). Unfortunately, even when using microelectrodes, data obtained at fast scan rates are still influenced by *IR* drop effects and the charging current so the positions of the oxidation and reduction peaks were found to be a function of both the scan rate and the electrode size. If a very fast scan rate is used, the resolution between processes 1 and 2 is decreased. Despite these limitations, at scan rates in excess of 5 V s^{-1} (dependent upon electrode size) it could be demonstrated that a reduction response on

the reverse scan of a cyclic voltammogram is observed at -0.23 V versus Fc$^+$/Fc which is attributed to the reduction of the short-lived seventeen-electron species *mer*-[W(CO)$_3$(η^1-dpm)(η^2-dpm)]$^+$ to *mer*-W(CO)$_3$(η^1-dpm)(η^2-dpm). *mer*-[W(CO)$_3$(η^1-dpm)(η^2-dpm)]$^+$ may also be oxidised at more positive potentials to [W(CO)$_3$(η^2-dpm)$_2$]$^{2+}$ as in process 2. Additionally, at fast scan rates a modified response is observed for the reduction of [W(CO)$_3$(η^2-dpm)$_2$]$^{2+}$. Unlike the case with the macroelectrode at slow scan rates (Fig. 1(a)), the reduction process of [W(CO)$_3$(η^2-dpm)$_2$]$^{2+}$ now has an associated one-electron oxidation step at -0.95 V versus Fc$^+$/Fc (Fig. 3). The reduction of [W(CO)$_3$(η^2-dpm)$_2$]$^{2+}$ is therefore concluded to occur as in eqn. (7)

$$[W(CO)_3(\eta^2\text{-dpm})_2]^{2+} + e^- \rightleftharpoons$$
$$[W(CO)_3(\eta^2\text{-dpm})_2]^+ \quad (7a)$$

$$[W(CO)_3(\eta^2\text{-dpm})_2]^+ \longrightarrow$$
$$mer\text{-}[W(CO)_3(\eta^1\text{-dpm})(\eta^2\text{-dpm})]^+ \quad (7b)$$

$$mer\text{-}[W(CO)_3(\eta^1\text{-dpm})(\eta^2\text{-dpm})]^+ + e^- \rightleftharpoons$$
$$W(CO)_3(\eta^1\text{-dpm})(\eta^2\text{-dpm}) \quad (7c)$$

The nineteen-electron [W(CO)$_3$(η^2-dpm)$_2$]$^+$ species rapidly changes to the seventeen-electron [W(CO)$_3$(η^1-dpm)(η^2-dpm)]$^+$ (eqn. (7b)) which is then immediately reduced to the starting material (eqn. (7c)) because the potential is more negative than that for eqn. (4a). At very fast scan rates reaction (7b) does not occur on the voltammetric time scale and a single one-electron process (eqn. (7a)) is observed and the fast scan data provides the first direct evidence for the existence of a nineteen-electron [W(CO)$_3$(η^2-dpm)$_2$]$^+$ species. It will be noted that eqns. (4b) and (7b) are the same equation reversed. The data imply that the reaction is fast in both directions which is not surprising since the
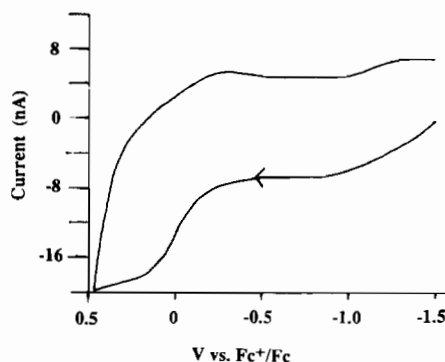

Fig. 3. Second scan of an oxidative cyclic voltammogram for a 0.5 mM solution of *mer*-W(CO)$_3$(η^1-dpm)(η^2-dpm) in acetone (0.1 M Et$_4$NClO$_4$) at a 12.5 μm radius platinum disc microelectrode (scan rate = 100 V s^{-1}).

676

reactions involve interconversion of seventeen-electron and nineteen-electron compounds. In both eqns. (4) and (7) there is a thermodynamic driving force in the preferred direction of oxidation or reduction.

Voltammetry at mercury electrodes

Figure 4(a) shows a polarogram obtained for the oxidation of mer-W(CO)$_3$(η^1-dpm)(η^2-dpm) in acetone and Fig. 4(b) shows the steady-state response at a 24 μm radius mercury microelectrode (scan rate 0.1 V s^{-1}) for the same solution. Figure 4(a) demonstrates that at a conventionally sized mercury electrode the polarographic steady-state response consists of two processes. The ratio of the currents for processes 1 and 2 at the mercury microelectrode of radius 24 μm approaches that at a 3 μm radius platinum microelectrode. This difference at mercury is attributed to the interaction of the pendent phosphorus atom of W(CO)$_3$(η^1-dpm)(η^2-dpm) with the mercury electrode, effectively slowing the apparent rate of the chelation reaction mer-[W(CO)$_3$(η^1-dpm)(η^2-dpm)]$^+$ → [W(CO)$_3$(η^2-dpm)$_2$]$^+$ (eqn. (4b)). The fast scan rate

(a)

V vs. Fc$^+$/Fc

(b)   V vs. Fc$^+$/Fc
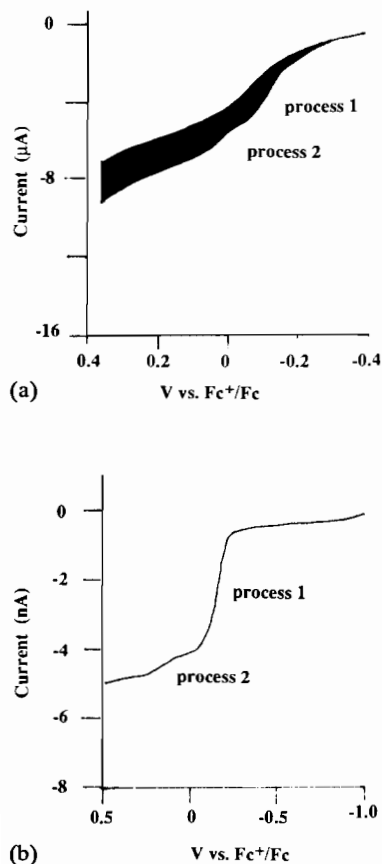
Fig. 4. Mercury electrode response for oxidation of a 0.5 mM solution of mer-W(CO)$_3$(η^1-dpm)(η^2-dpm) in acetone (0.1 M Et$_4$NClO$_4$) at (a) a dropping mercury electrode (drop time = 0.5 s), (b) a 24 μm radius mercury microelectrode (scan rate = 0.1 V s^{-1}).
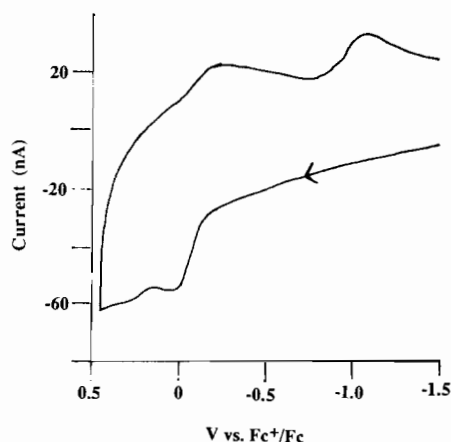
Fig. 5. Oxidative cyclic voltammogram for a 0.5 mM solution of mer-W(CO)$_3$(η^1-dpm)(η^2-dpm) in acetone (0.1 M Et$_4$NClO$_4$) at a 24 μm radius mercury microelectrode at a scan rate of 150 V s^{-1}.

data observed at mercury microelectrodes (Fig. 5) leads to easy observation of intermediates the same as those identified from fast scan rate cyclic voltammetry at platinum microelectrodes.

Conclusions

This study of the electrochemical oxidation of mer-W(CO)$_3$(η^1-dpm)(η^2-dpm) demonstrates the value of using voltammetry at microelectrodes of different materials under both steady-state (low scan rates, radial diffusion dominant) and transient (fast scan rate, linear diffusion dominant) regimes. Under steady-state conditions with a very small platinum electrode, two one-electron steps are detected at low scan rates rather than a single two-electron process observed under conventional conditions (large electrode). Under transient conditions at a platinum microelectrode considerable information may be gleaned about reactive intermediates, such as the identification of mer-[W(CO)$_3$(η^1-dpm)(η^2-dpm)]$^+$ and [W(CO)$_3$(η^2-dpm)$_2$]$^+$. However, the large IR drop and charging current effects are disadvantages of the fast scan method. Both steady-state and transient voltammetry show that chelation of the pendent phosphorus group occurs after each electron transfer step and that interaction with a mercury electrode slows the apparent rate of this step.

Acknowledgements

References

1 F. A. Wimmer, M. R. Snow and A. M. Bond, *Inorg. Chem.*, *13* (1974) 1617.

2 A. M. Bond, R. Colton and J. J. Jackowski, *Inorg. Chem.*, *14* (1975) 274.

3 A. M. Bond and R. Colton, *Inorg. Chem.*, *15* (1976) 2036.

4 A. M. Bond, R. Colton and M. J. McCormick, *Inorg. Chem.*, *16* (1977) 155.

5 R. N. Bagchi, A. M. Bond, G. Brain, R. Colton, T. L. E. Henderson and J. Kevekordes, *Organometallics*, *3* (1984) 4.

6 A. Blagg, S. W. Carr, G. R. Cooper, I. D. Dobson, J. B. Gill, D. C. Goodall, B. L. Shaw, N. Taylor and T. J. Boddington, *J. Chem. Soc., Dalton Trans.*, (1985) 1213.

7 A. M. Bond, R. Colton and K. McGregor, *Inorg. Chem.*, *25* (1986) 2378.

8 A. M. Bond, R. Colton and J. J. Jackowski, *Inorg. Chem.*, *18* (1979) 1977.

9 A. M. Bond, S. W. Carr and R. Colton, *Organometallics*, *23* (1984) 541.

10 A. M. Bond, S. W. Carr and R. Colton, *Inorg. Chem.*, *23* (1984) 2343.

11 A. M. Bond, R. Colton, S. W. Feldberg, P. J. Mahon and T. Whyte, *Organometallics*, *10* (1991) 3320.

12 A. Blagg, G. R. Cooper, P. G. Pringle, R. Robson and B. L. Shaw, *J. Chem. Soc., Chem. Commun.*, (1984) 933.

13 J. W. Bixler, A. M. Bond, P. A. Lay, W. Thormann, P. Van den Bosch, M. Fleischmann and B. S. Pons, *Anal. Chim. Acta*, *187* (1986) 67.

14 B. Scharifker and G. Hills, *J. Electroanal. Chem.*, *130* (1981) 81.

15 Y. Saito, *Rev. Polarogr.*, *15* (1968) 177.

16 A. M. Bond, M. Fleischmann and J. Robinson, *J. Electroanal. Chem.*, *168* (1984) 299.

17 A. M. Bond, R. Colton and K. McGregor, *Organometallics*, *9* (1990) 1227.

18 S. W. Feldberg and L. Jeftic, *J. Phys. Chem.*, *76* (1972) 2439.

19 M. Fleischmann, F. Lasserre, J. Robinson and D. Swan, *J. Electroanal. Chem.*, *177* (1984) 97.

20 M. Fleischmann, F. Lasserre and J. Robinson, *J. Electroanal. Chem.*, *177* (1984) 115.